Nat. Hazards Earth Syst. Sci., 14, 2649–2653, 2014
www.nat-hazards-earth-syst-sci.net/14/2649/2014/
doi:10.5194/nhess-14-2649-2014

Natural Hazards and Earth System Sciences
Open Access

Brief Communication: The interaction of clouds with surface latent heat flux variation before the 2011 $M = 6.1$ Russia earthquake

Y. Jie and G. Guangmeng

Remote Sensing Center, Nanyang Normal University, Nanyang, China

Correspondence to: G. Guangmeng (guogm@igsnrr.ac.cn)

Received: 12 November 2013 – Published in Nat. Hazards Earth Syst. Sci. Discuss.: 17 January 2014
Revised: 1 September 2014 – Accepted: 17 September 2014 – Published: 29 September 2014

Abstract. Recently, surface latent heat flux (SLHF) data have been widely used to study the anomalies before earthquakes. Most studies use the daily SLHF data. Here we use both the daily SLHF data and the high temporal resolution (four times one day) SLHF data, and compare the SLHF changes with satellite cloud images at the first time. We check the data from 1 September to 30 October 2011, and the result shows that there is really a very high SLHF anomaly (more than 2σ) in the epicenter area just 5 days before the $M = 6.1$ Russia earthquake that occurred on 14 October 2011. It should be considered as a preseismic precursor if judged with previously published methods, but our comparison between SLHF change and satellite images shows that the SLHF anomaly is contaminated by a thick cloud. It is difficult to verify that this SLHF anomaly is caused by an earthquake and our analysis shows that it is more related to meteorological reason. This example tells us that scientists must know the data's meaning before they use it; if not, they may draw a wrong conclusion. Based on this example, we suggest that previously published SLHF anomalies before earthquakes should be reanalyzed with our method to exclude the false anomalies.

1 Introduction

Earthquake is the result of stress increase and rock fracture. According to some scholars (Friedemann et al., 2009), prior to an earthquake the stress accumulation results in a thermal infrared emission. Though until now this has not been widely accepted, many papers on thermal anomalies preceding earthquakes have been published, such as preseismic thermal anomalies in China (10 January 1998) (Qiang et al., 1991; Tronin, 2000) and Japan (17 January 1995) (Tronin et al., 2002), Algeria (Saraf and Choudhury, 2004), Turkey (Tramutoli et al., 2005), and Italy (Qin et al., 2012a). The thermal emission will enhance the rate of energy exchange between surface and atmosphere, and leads to an increase in surface latent heat flux (SLHF). SLHF is the heat released by phase changes due to evaporation or melting. The energy transport between the earth, ocean and atmosphere through the evaporation at the surface–atmosphere interface partly compensates for energy losses due to radiation processes in the atmosphere (Schulz et al., 1997). The energy losses at the surface through simultaneous exchange of water vapor and heat with the atmosphere are higher at the ocean surface compared to those over the land; hence SLHF is always higher at the ocean surface and lower in the land area.

The SLHF can be retrieved accurately from satellite data (Schulz et al., 1997), which provides an opportunity for long-term monitoring of the parameter. Dey and Singh (2003) analyzed the daily SLHF from the epicenter regions of five recent earthquakes that occurred close to the oceans, and found a maximum increase of SLHF 2–7 days prior to the main earthquake event. They considered that this increase is likely due to an ocean–land–atmosphere interaction and the anomalous behavior of SLHF is only associated with the coastal earthquakes. Qin et al. (2011, 2012b, 2014) analyzed the daily SLHF anomalies before the $M_s = 7.1$ New Zealand earthquake and the Pu'er earthquake of China. Xu et al. (2011) and Cervone et al. (2006) analyzed the SLHF anomalies before the $M = 9.0$ Sendai earthquake on 11 March 2011 and the $M = 8.3$ earthquake on 25 September 2003 in Japan. In all of these studies, the temporal resolution of SLHF data is on a daily basis. Here we analyze SLHF data variation preceding Russia's $M = 6.1$ earthquake with

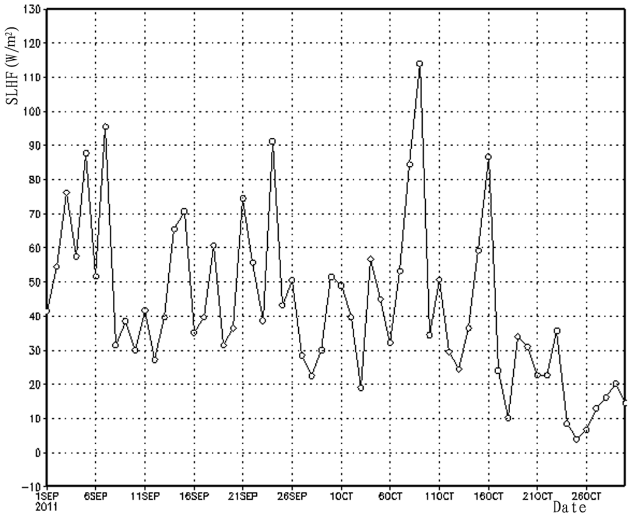

Figure 1. Daily SLHF time series of the epicenter grid from 1 September to 30 October 2011, where a clear sharp increase appeared on 9 October.

high temporal resolution data observed four times per day, and cast some doubts on the previously found results.

2 Data

The SLHF data are provided by the National Center for Environmental Prediction (NCEP) of NOAA. The NCEP/NCAR Reanalysis project uses a state-of-the-art analysis system to perform data assimilation using past data from 1948 to the present. It provides four time measurements at 00:00, 06:00, 12:00, and 18:00 UTC everyday, and its spatial coverage is 0–358.125° E, 88.542 N–88.542° S, with a total of 192×94 points (Kalnay et al., 1996).

The $M = 6.1$ earthquake occurred at 06:10 UTC on 14 October 2011 at 54.1° N, 123.7° E with a focal depth of 12 km, which was registered close to Russia's southeastern border with China. It occurred in high latitude areas that have fewer earthquakes than mid- to low-latitude areas. This quake is the only one that exceeds $M = 5.0$ on the Richter scale in the area 50–55° N, 120–125° E in the last 50 years. Thus, it is a very rare event. It is about 720 km to the closest coast, but there are many lakes and rivers in this area because it is in the high latitude and the weather is cold and wet. The multi-year mean temperature in 54° N, 124° E in October is −4° C.

3 Method and result

First, we extract the daily SLHF data at the epicenter point, and plot the time series from 1 September to 30 October 2011. We can see from Fig. 1 that the SLHF on 9 October is the maximum.

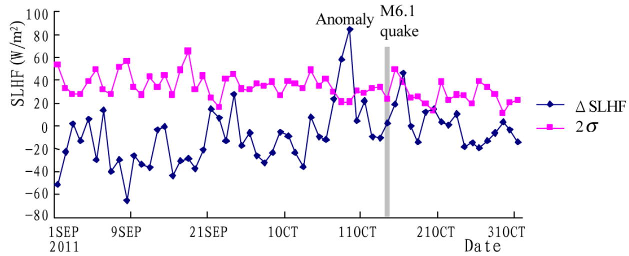

Figure 2. SLHF daily change from 1 September to 31 October 2011 compared with the 2σ curve during the last 10 years, revealing a clear anomaly bigger than 2σ that appeared on 9 October, just 5 days before the $M = 6.1$ quake.

Second, we subtract the daily SLHF from the multi-year mean values that represent the normal background, to get ΔSLHF as given by Qin et al. (2011):

$$\Delta\text{SLHF} = \text{SLHF}_{\text{EQ}} - \frac{1}{n}\sum_{i=1}^{n}\text{SLHF}_i, \quad (1)$$

where SLHF_{EQ} is the daily SLHF of 2011, SLHF_i is the corresponding daily SLHF for 2001–2010, and n is the number of years analyzed, i.e., 10 (Qin et al., 2011). We analyze the long time series of SLHF data on the epicentral pixel (54.1° N, 123.7° E). For the comparison of the data for 2011 with historical data, the mean (μ) and standard deviation (σ) are also calculated using the multi-year (2001–2010) data on the same day. The result is listed in Fig. 2, and we can see that a clear anomaly appeared on 9 October.

Third, we plot the SLHF data with 6-hour resolution to get a detailed analysis (Fig. 3). The data show that the maximum SLHF is at 00:00 UTC on 9 October. This is an important point that is different from previous research, and we will address this in detail in the following text.

Finally, we plot the spatial distribution map at 00:00 UTC 9 October (Fig. 4). The spatial distribution of the SLHF anomaly prior to the main shock is studied in the 40° by 20° area (about 8 000 000 km^2) around the epicenter, and we can see that there are two areas with high SLHF value: one is located at 47° N, 136° E on the ocean–land border, and maybe the high value herein is caused by ocean, and the other is at 54° N, 124° E, which is located in the epicenter exactly. Therefore, maybe the second area with high SLHF is related to the earthquake on 14 October. From Fig. 2 we can see that there is a maximum SLHF on 9 October, just 5 days before the quake; from the spatial map, we can see that the maximum SLHF is located in the epicenter exactly. This conclusion agrees apparently well with Dey and Singh's result (2003), and when people see this result, most of them will consider it an earthquake precursor.

The maximum SLHF data are at 00:00 UTC, so we check the satellite data at 00:00 UTC on 9 October (Fig. 5). The satellite image shows that there is a thick cloud at the epicenter area, and this thick cloud is continuously moving from

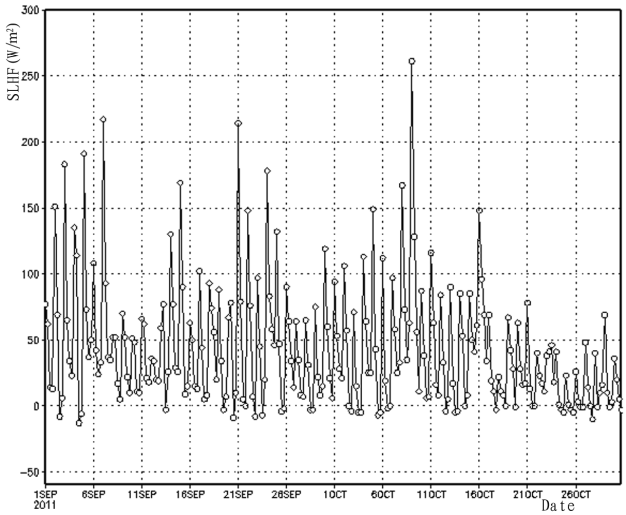

Figure 3. SLHF time series of the epicenter grid with 6 h resolution from 1 September to 30 October 2011, where the maximum SLHF is shown at 00:00 UTC on 9 October.

0Z to 6Z (see Fig. 6). In Fig. 4, we notice that in correspondence to the cloud at 55° N, 135° E, there is an SLHF value less than 100 W m^{-2}, and it is much less than that at 54° N, 124° E. This means that clouds do not always increase SLHF value. SLHF is mainly controlled by wind speed and temperature (Qin et al., 2011), so we check the weather data, and find that

1. The weather station at 54° N, 123.9° E is located in the epicenter area that recorded 5 mm rainfall on 9 October 2011. Hence, a high SLHF here is normal and reasonable.

2. In the epicenter area, the V wind changed from 4 m s^{-1} at 1000 hpa to 13 m s^{-1} at 850 hpa, which means a strong vertical convection. There are also thick clouds at 55° N, 135° E. The wind change there is about 2 to 4 m s^{-1} from 1000 to 850 hpa. It is small, so there is no high SLHF value there.

3. Observed from the satellite visible band image, clouds in the epicenter area have some rises and falls, which mean high convection. This shows that this cloud is undergoing a very intense phase change due to condensation and that a large amount of energy is released (Schulz et al., 1997). The cloud at 55° N, 135° E is very homogeneous, which means little convection, so a low SLHF value at 55° N, 135° E is reasonable.

4. Even after the thick clouds move away from the epicenter area, there are still many thin clouds and fog left in the epicenter area. In the SLHF data, there are many examples showing that the high SLHF area does not move within 6 h and that no quakes ensued. Therefore, the phenomenon about stationary SLHF within 6 h is very common.

5. Lifted index (LI) is the temperature difference between an air parcel lifted adiabatically and the temperature of the environment at a given pressure height in the troposphere. When the value is positive, the atmosphere is stable, and when the value is negative, the atmosphere is unstable. Here we calculate the correlation between SLHF and LI. It is -0.30 at 00Z and -0.42 at 06Z. This shows that high SLHF occurred in unstable atmosphere areas. The correlation between SLHF and CPR (convective precipitation rate) is also calculated on 9 October; it is 0.26 at 00:00 UTC and 0.31 at 06:00 UTC.

6. We find that the ΔSLHF on 14 October 2004 is also bigger than 2σ compared with the same time from 2001 to 2010, and it also exists in a localized area, while no quakes bigger than $M = 5.0$ happened in the following 3 months.

7. We also check the total electron content (TEC) of the ionosphere and find no anomaly. This means that there is no lithosphere–atmosphere–ionosphere coupling before this quake.

According to these seven pieces of evidence, we consider that the anomalous SLHF variation is more related to weather changes, not earthquake. Zhang et al. (2013) also gives a similar conclusion after analyzing six strong quakes. However, strictly speaking, how the earthquakes interact with SLHF is still unknown, so we can not totally exclude the possibility that the anomalous SLHF might be related to an earthquake. This needs more detailed weather data and geophysical data, such as the local radon data, and some new methods should be developed to distinguish whether the SLHF is caused by weather or by earthquake. This also shows that under current conditions, there is still controversy about the SLHF precursors, which have not been widely accepted.

In this example, we consider that cloud contamination is a problem that must be taken into account. Here we report such an issue and remind researchers that we cannot always take apparent anomalies at face value. Previous studies just plot the SLHF data and use mathematical methods to compare the SLHF data with the background. If the data are above the threshold, it can be considered as an anomaly. However, they did not point out whether the atmospheric weather is clear or cloudy. Here, after checking the satellite data and the weather data, we find that the high SLHF is likely contaminated by a thick cloud. Because of the limited data, we do not know whether this cloud is related to the quake. If it is, then it means cloud activity can be affected by earthquake activity, as Morozova (1997) and Shou (1999) discovered. If it is not, that means the weather change can lead to SLHF variation, and this will be misunderstood sometimes. Whatever it is, this example shows that no matter how complex

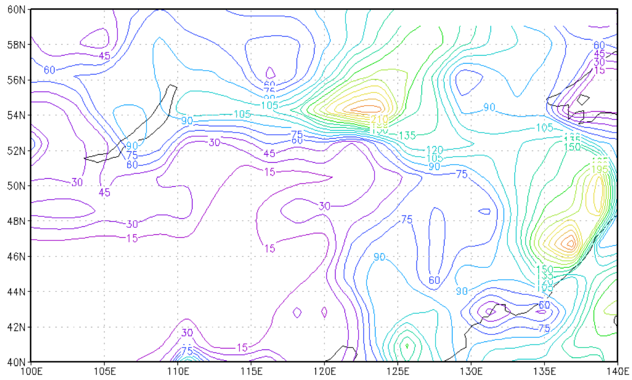

Figure 4. SLHF spatial map at 00:00 UTC on 9 October, showing a high SLHF (unit: $W\,m^{-2}$) area located exactly in the epicenter area at 54.1° N, 123.7° E.

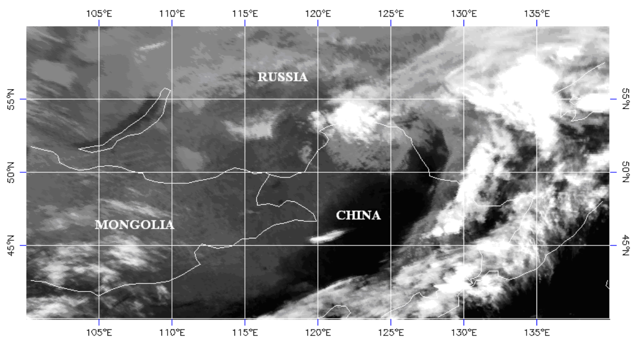

Figure 5. Satellite image of Russia and northeastern China at 00:00 UTC on 9 October 2011. The area is the same as Fig. 4; a thick cloud appears in the 53–55° N, 121–124° E epicenter area.

and how advanced the method is, such as wavelet transform, principal component analysis, neural network and so on, it is important to know what the data mean before being used, or one will get a wrong conclusion.

4 Conclusions

We analyze the daily and 6-hourly SLHF data preceding the $M = 6.1$ Russian earthquake. It is found that the SLHF data reached the maximum 5 days before the quake, which is also the biggest value from 1 September to 30 October, and that the high SLHF area is located in the epicenter exactly. All these results are well in accordance with those published previously, but when checking the SLHF data with 6 h resolution, we find that the maximum SLHF value appeared at 00:00 UTC. This high temporal resolution makes it possible that we can check the satellite data at the same time with SLHF data. We find that there is a thick cloud existing in the high SLHF area. With the weather data and the satellite data, we infer that the anomalous SLHF variation is more related to weather changes, but, strictly speaking, we can not totally

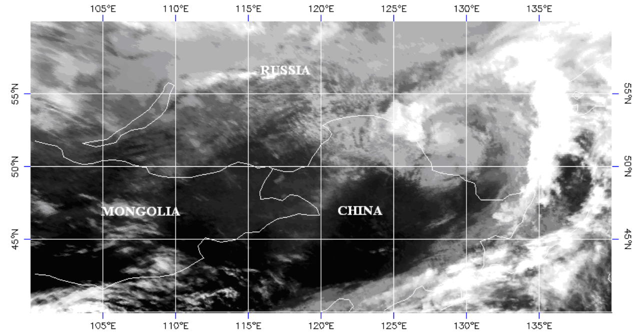

Figure 6. Satellite image of Russia and northeastern China at 06:00 UTC on 9 October 2011. The area is the same as Fig. 4, and we can see the thick cloud has moved to 53–54° N, 125–127° E.

exclude the possibility that the anomalous SLHF might be related to an earthquake. This uncertainty also shows there is still controversy about SLHF precursors that have not been widely accepted. Therefore, we suggest that before using the data, researchers have to understand what the data mean; if not, they are likely to get a wrong conclusion, for example considering normal SLHF change as earthquake precursors.

A similar situation is the research on preseismic thermal anomaly. Blackett et al. (2011) checked the land surface temperature (LST) data and methods, and found that some anomalies were caused by the presence of a MODIS LST data gap, which was attributed to cloud cover and a mosaic of neighboring orbit data. Here our research shows a similar conclusion. This is more important in this big data era, because some famous organizations such as NASA and NOAA provide thousands of satellite data products every year, and as a result, the data volume is too big and the data production process is so complex that few people know every step of the data production. Especially in earthquake precursor research, geologists try to use the data from meteorological satellite data, which is an inter-disciplinary area that is liable to have more chance of being wrong. Therefore, it is highly recommended that previously published papers on SLHF be reanalyzed with simultaneous satellite data and weather data to exclude possible false precursors.

Acknowledgements. This work was supported by NSFC project 41071280. The NCEP data were provided by the NOAA/OAR/ESRL PSD, Boulder, Colorado, USA. Their help is greatly appreciated. We also thank M. Blackett and A. De Santis for their invaluable suggestions.

Edited by: B. D. Malamud
Reviewed by: M. Blackett and A. De Santis

References

Blackett, M., Wooster, M. J., and Malamud, B. D.: Exploring land surface temperature earthquake precursors: A focus on the Gujarat (India) earthquake of 2001, Geophys. Res. Lett., 38, L15303, doi:10.1029/2011GL048282, 2011.

Cervone, G., Maekawa, S., Singh, R. P., Hayakawa, M., Kafatos, M., and Shvets, A.: Surface latent heat flux and nighttime LF anomalies prior to the $M_w = 8.3$ Tokachi-Oki earthquake, Nat. Hazards Earth Syst. Sci., 6, 109–114, doi:10.5194/nhess-6-109-2006, 2006.

Dey, S. and Singh, R. P.: Surface latent heat flux as an earthquake precursor, Nat. Hazards Earth Syst. Sci., 3, 749–755, doi:10.5194/nhess-3-749-2003, 2003.

Friedemann, T. F., Kulahci, I. G., Gary, C., Ling, J. L., Winnick, M., Tregloan-Reed, J., and Freund, M. M.: Air ionization at rock surfaces and pre-earthquake signals, J. Atmos. Solar-Terrest. Phys., 71, 1824–1834, 2009.

Kalnay, E., Kanamitsu, M., Kistler, R., Collins, W., Deaven, D., Gandin, L., Iredell, M., Saha, S.,White, G., Woollen, J., Zhu, Y., Leetmaa, A., Reynolds, R., Chelliah, M., Ebisuzaki, W., Higgins, W., Janowiak, J., Mo, K. C., Ropelewski, C., Wang, J., Jenne, R., and Joseph, D.: The NCEP/NCAR 40-year reanalysis project, Bull. Am. Meteorol. Soc., 77, 437–470, 1996.

Morozova, L. I.: Dynamics of cloudy anomalies above fracture regions during natural and anthropogenically caused seismic activities, Fizika Zemli, 9, 94–96, 1997.

Qiang, Z. J., Xu, X. D., and Dian, C. G.: Thermal infrared anomaly precursor of impending earthquakes, Chin. Sci. Bull., 36, 319–323, 1991.

Qin, K., Wu, L. X., De Santis, A., and Wang, H.: Surface latent heat flux anomalies before the Ms7.1 New Zealand earthquake 2010, Chinese Sci. Bull., 56, 3273–3280, 2011.

Qin, K., Wu, L. X., De Santis, A., and Cianchini, G.: Preliminary analysis of surface temperature anomalies preceding the two major 2012 Emilia (Italy) earthquakes, Ann. Geophys., 55, 823–828, 2012a,
http://www.ann-geophys.net/55/823/2012/.

Qin, K., Wu, L. X., De Santis, A., Meng, J., Ma, W. Y., and Cianchini, G.: Quasi-synchronous multi-parameter anomalies associated with the 2010–2011 New Zealand earthquake sequence, Nat. Hazards Earth Syst. Sci., 12, 1059–1072, doi:10.5194/nhess-12-1059-2012, 2012b.

Qin, K., Wu, L. X., Ouyang, X. Y., Shen, X. H., and Zheng, S.: Surface latent heat flux anomalies quasi-synchronous with ionospheric disturbances before the 2007 Pu'er earthquake in China, Adv. Space Res., 53, 266–271, 2014.

Saraf, A. K. and Choudhury, S.: Satellite detects surface thermal anomalies associated with the Algerian earthquakes of May 2003, Int. J. Remote Sens., 26, 2705–2713, 2004.

Schulz, J., Meywerk, J., and Ewald, S.: Evaluation of satellite-derived latent Heat Fluxes, J. Climate, 10, 2782–2795, 1997.

Shou, Z. H.: Earthquake Clouds, a reliable precursor, Science & Utopya, 64, 53–57, 1999.

Tronin, A. A.: Thermal IR satellite sensor data application for earthquake research in China, Int. J. Remote Sens., 21, 3169–3177, 2000.

Tronin, A. A., Masashi Hayakawa, and Molchanov, O. A.: Thermal IR satellite data application for earthquake research in Japan and China, J. Geodynam., 33, 519–534, 2002.

Tramutoli, V., Cuomo, V., and Filizzola, B.: Assessing the potential of thermal infrared satellite surveys for monitoring seismically active areas: the case of Kocaeli (Izmit) earthquake, 17 August 1999, Remote Sens. Environ., 96, 409–426, 2005.

Xu, T., Chen, Z., Li, C. B., Wu, J., Hu,Y. L., and Wu, Z. S.: GPS total electron content and surface latent heat flux variations before the 11 March 2011 $M9.0$ Sendai earthquake, Adv. Space Res., 48, 1311–1317, 2011.

Zhang, W., Zhao, J., Wang, W., Ren, H., Chen, L., and Yan, G.: A preliminary evaluation of surface latent heat flux as an earthquake precursor, Nat. Hazards Earth Syst. Sci., 13, 2639–2647, doi:10.5194/nhess-13-2639-2013, 2013.